ICANS IX

INTERNATIONAL COLLABORATION ON ADVANCED NEUTRON SOURCES

22-26 September, 1986

Deterioration of Performance of Neutron Moderators Under Intense Irradiation*

John M. Carpenter,

Scott S. Cudrnak[a]

and

Casimer M. DeCusatis[b]

Intense Pulsed Neutron Source Program
Argonne National Laboratory
Argonne, Illinois 60439 U.S.A.

ABSTRACT

In pulsed neutron sources, fixed moderators such as polyethylene and solid methane slow down fast (MeV) neutrons from the primary source to energies of use for spectroscopy ($\lesssim$ 10 eV). Radiation-induced changes in their composition alter their spectral and pulse characteristics. We report the results of fitting time-average spectra from polyethylene and solid methane moderators in Argonne's Intense Pulsed Neutron Source as a function of total fast-neutron radiation dose. The thermal-to-epithermal flux ratio varies most significantly, while the Maxwellian energy and the parameters describing the epithermal component change only slightly. We have used modified forms of Westcott's joining function for this purpose. We provide an integral of the spectrum that is useful for determining the delayed neutron background.

Introduction

In pulsed neutron sources, fixed moderators such as polyethylene and solid methane slow down fast (MeV) neutrons from the primary source to energies of use for spectroscopy ($\lesssim$ 10 eV). Radiation-induced changes in

Work Supported by U.S. Department of Energy

a) Present address: Department of Civil Engineering, Mechanics, and Metallurgy, University of Illinois at Chicago, Chicago, IL

b) Present address: Department of Engineering Science and Mechanics, Pennsylvania State University, University Park, PA

their composition alter the spectral and pulse characteristics of moderators. The purpose of this work is to quantify the changes in the parameters describing the time-average spectrum of neutrons from the moderators of Argonne's Intense Pulsed Neutron Source[1] (IPNS) by fitting empirical functions to observed time-of-flight spectra. The results relate to other pulsed sources which use polyethylene or solid methane moderators. It is particularly significant that simple functions of the same mathematical form, but differing for polyethylene and methane, fit the spectra equally well at all stages of their irradiation.

We find that in polyethylene suffering about $5 \times 10^{18} n/cm^2$ fast neutron fluence, both the thermal-to-epithermal neutron flux ratio and the ratio of epithermal flux to the proton current, both decrease by a factor of about .75. These changes are important, but not unique to pulsed sources, since fluxes and spectra also change by comparable factors from beginning to end of the fuel cycle in some reactors, due to fuel burnup and the changing positions of shim rods. Similarly, we find that the thermal-to-epithermal flux ratio in methane decreases by a factor of about .80 upon irradiation by $8 \times 10^{17} n/cm^2$, while the ratio of epithermal flux to proton current decreases by only .95.

Description of the Moderators and the Measurements

Figure 1 shows the arrangement of the primary source, moderators and reflector of the IPNS. The source (proton target) is of depleted Uranium, irradiated by 450 MeV protons from the Rapid Cycling Synchrotron (RCS). During the period we investigated, the accelerator delivered time-average currents of about 12 μA in pulses 100 nsec in duration at 30 Hz. Figures 2 and 3 show the moderators, which are respectively of polyethylene and solid methane. The moderators are decoupled from the surrounding graphite reflector by 0.5 mm-thick Cadmium. The physical temperature of the polyethylene moderators is about 50 C, and of the methane about 12 K during operation. Our measurements were of the "F" moderator, overall $5.1 \times 10.1 \times 10.1$ cm^3 in size, heterogeneously poisoned with 0.5 mm-thick Cadmium 2.2 cm below the viewed surface, and of the grooved, solid methane "C" moderator.

The polyethylene moderator was initially of high density material, $\rho = 0.966$ gm/cm^3, with H/C ratio 2.00. After approximately one year's irradiation, corresponding to $8. \times 10^{20}$ protons on target and a fast-neutron fluence approximately $5 \times 10^{18} n/cm^2$, the polyethylene moderator was removed and its composition examined. Table 1 summarizes the results of analysis of material from "F" moderator before and after irradiation.

IPNS-I NEUTRON SCATTERING EXPERIMENTAL ASSEMBLY

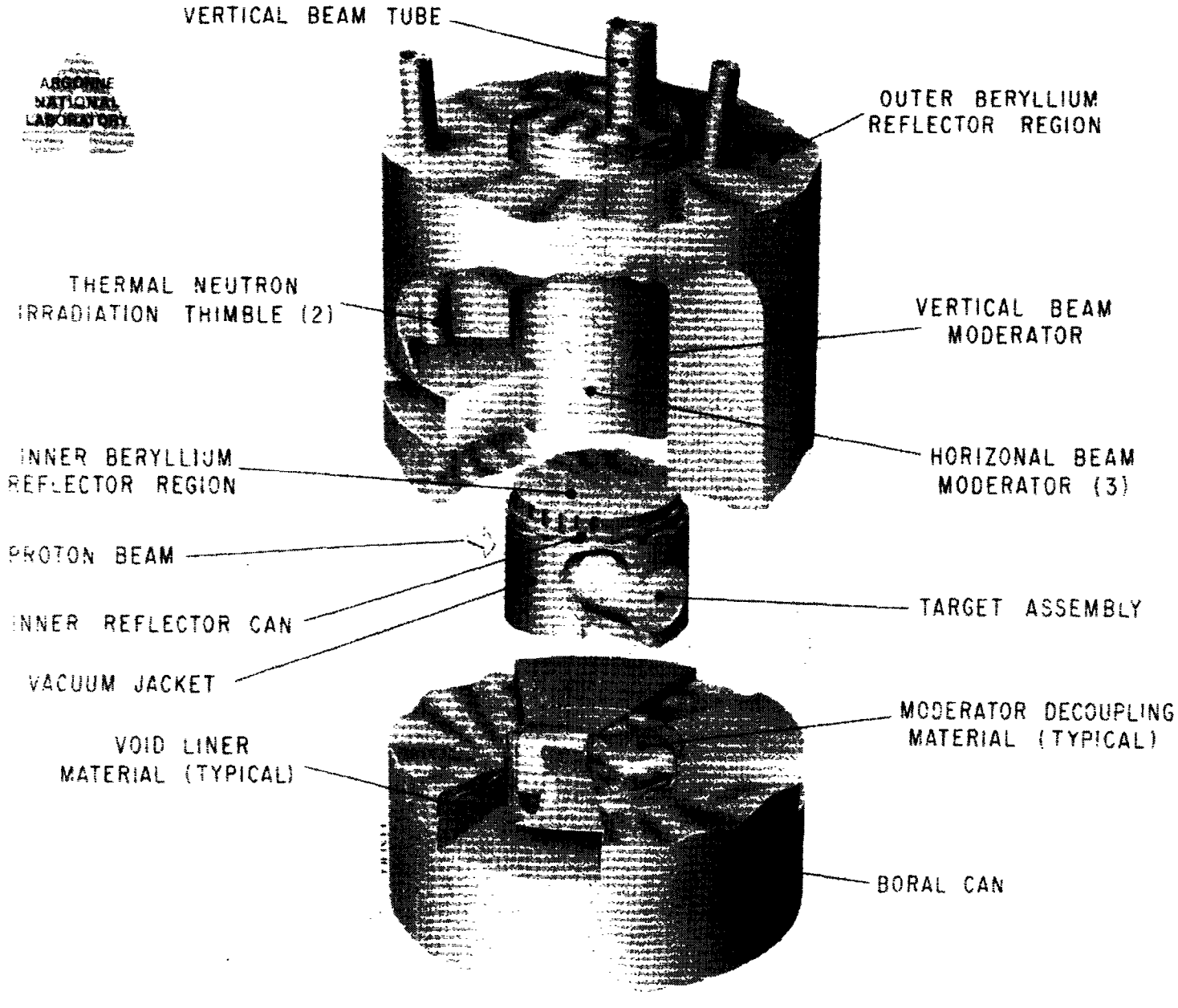

1. The IPNS Target Moderator Reflector system.

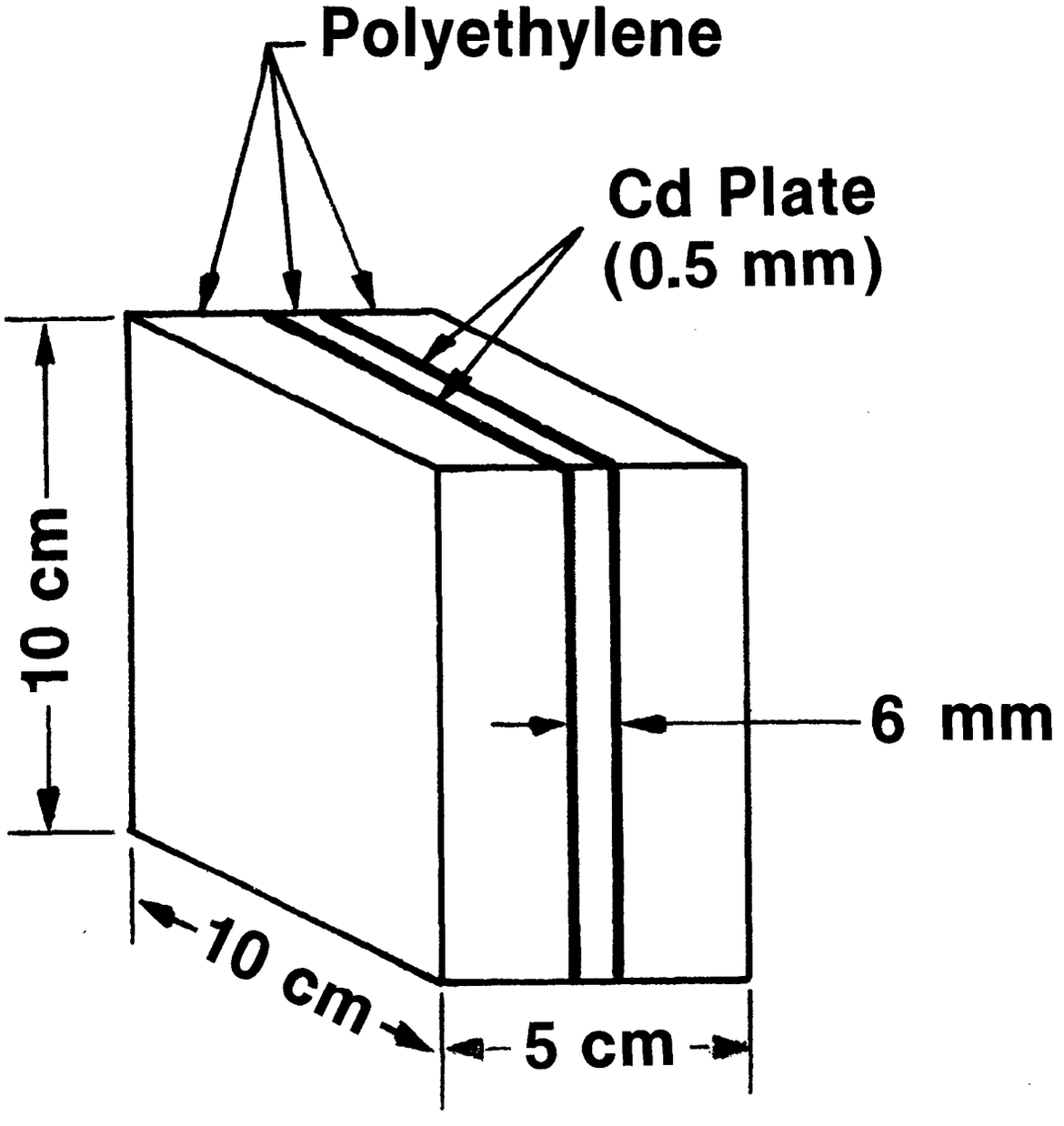

2. The IPNS ambient temperature polyethylene "F" moderator.

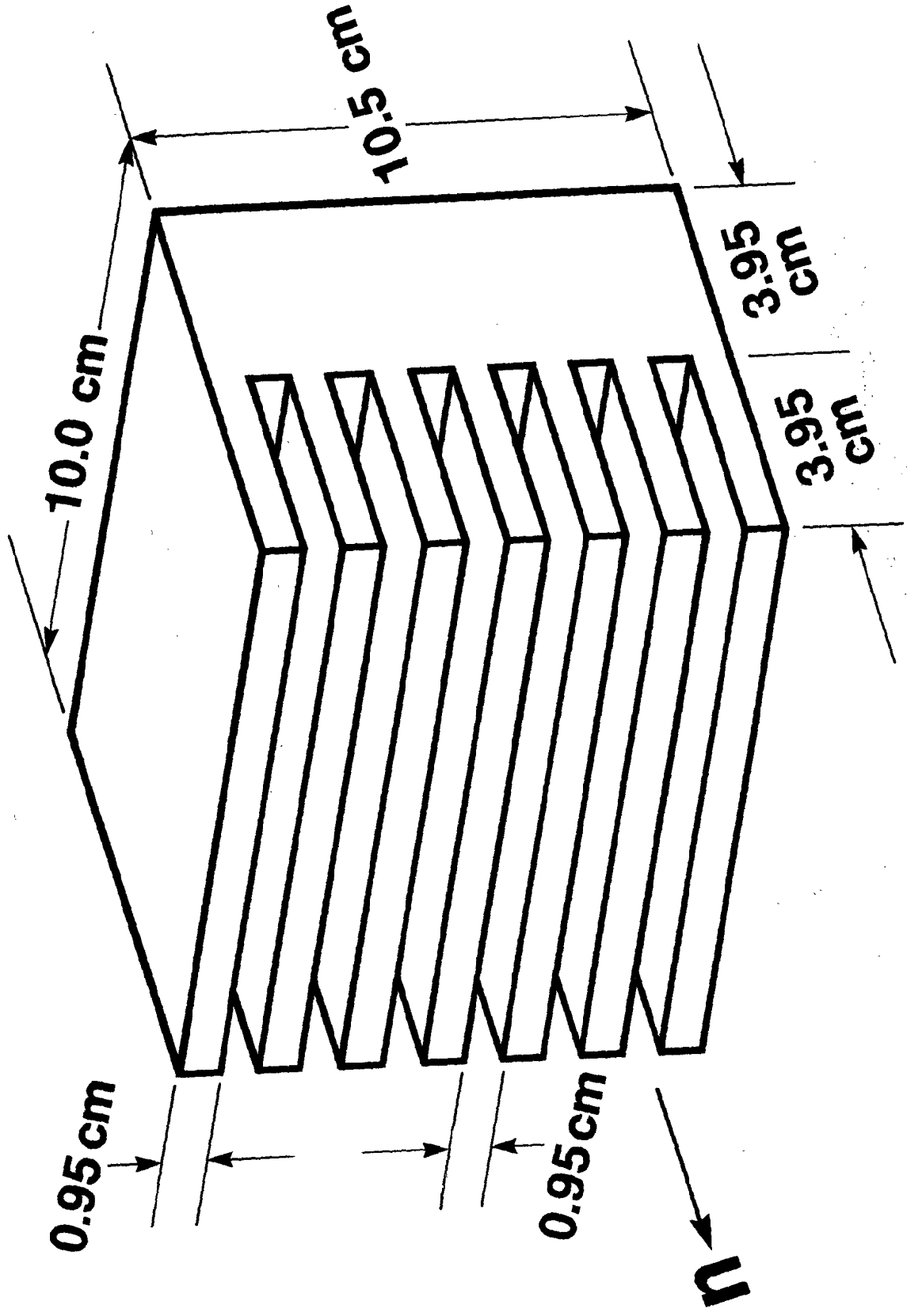

3. The IPNS grooved solid methane moderator.

Table 1

Analysis of Polyethylene Before and After Irradiation

	Before	After 8.1×10^{20} protons on target
Density	0.966	0.990 gm/cm^3
H/C ratio	2.0	1.56

The methane moderator consisted of initially pure (> 0.999) methane gas condensed into the methane container, which for heat transfer purposes contains a 6101 Aluminum alloy foam filling 6% of the volume. (The density of pure solid methane at 12 K is 0.528 gm/cm^3.) The system is described in greater detail elsewhere[2]. Following two periods of irradiation, one 15 days long and the other 55 days long, during which the RCS delivered 6.5×10^{19} and 3.3×10^{20} protons to the target, corresponding respectively to approximately $4. \times 10^{17}$ n/cm^2 and 2×10^{18} n/cm^2 fast neutron fluence in the methane, we collected and analyzed the volatile products, with the results shown in Table 2.

Table 2

Analysis of Volatile Products of Radiolysis of Methane from the IPNS Solid Methane Moderator

Product	Mole fraction* of product, %	
protons on target	6.5×10^{19}	3.3×10^{20}
H_2	5.38	10.6
CH_4	91.37	75.2
H_2O	<0.04	-
C_2H_4	0.20	1.4
C_2H_6	2.30	8.5
N_2	not determined--used as mixing gas	
O_2	0.17	1.4
Ar	0.04	0.1
C_3H_8	0.42	-
hydrocarbons C_3, C_4 & c	-	2.8

*exclusive of N_2.

These analyses indicate substantial deterioration of both CH_2 and CH_4 resulting from irradiation, which is reflected in the measured spectra described below.

Our estimates of the fast neutron fluence F are admittedly crude, and are based on treating the target as a point source of fast neutrons;

$$F = YN_p/(4\pi r^2), \tag{1}$$

where $Y \simeq 17$ neutrons per proton is the neutron yield, $r \simeq 15$ cm is the distance to the center of the moderator, and N_p is the number of protons delivered to the target.

Assuming the average neutron energy to be $E \simeq 1.$ MeV, and the proton cross section to be $\sigma \simeq 4$ barns/proton, with 1/2 the energy given to the proton in each collision, and taking $n = 8.3 \times 10^{22}$ protons/cm^3 to be the density of protons in the polyethylene, we arrive at an estimate of the neutron dose for 8×10^{20} protons on target,

$$D = \sigma Fn(E/2) = 2.3 \times 10^{12} \text{ erg/cm}^3 = 2.4 \times 10^{10} \text{ Rad.} \tag{2}$$

Similar crude estimates of the gamma ray dose lead to estimates about two orders of magnitude smaller than the neutron dose. Protons which might be present in the wings of the proton beam would contribute significantly to the dose, but we can only assert on the basis of measurements on the second target of IPNS, that this component is about two orders of magnitude smaller than the neutron dose.

Beam monitor detectors in two instruments, the Special Environment Powder Diffractometer (SEPD) viewing the ambient-temperature polyethylene moderator through beam port F5, and the Small Angle Diffractometer (SAD) viewing the solid methane moderator through beam port C1, provided the time-of-flight data which are the basis of our results. The detectors were both "thin" $^{10}BF_3$ detectors, whose efficiency is proportional to the neutron wavelength over the entire range of wavelengths (energies) measured. Figure 4 schematically shows the arrangement of the measurements. The flight path lengths were 13.51 m and 6.38 m for the SEPD and SAD beam monitor detectors, respectively. We have included a small correction to the flight path lengths to account approximately for the emission time delay.

The Fitting Functions

The time-average counting rate per unit time-of-flight in a pulsed-source beam monitor spectrum measurement is

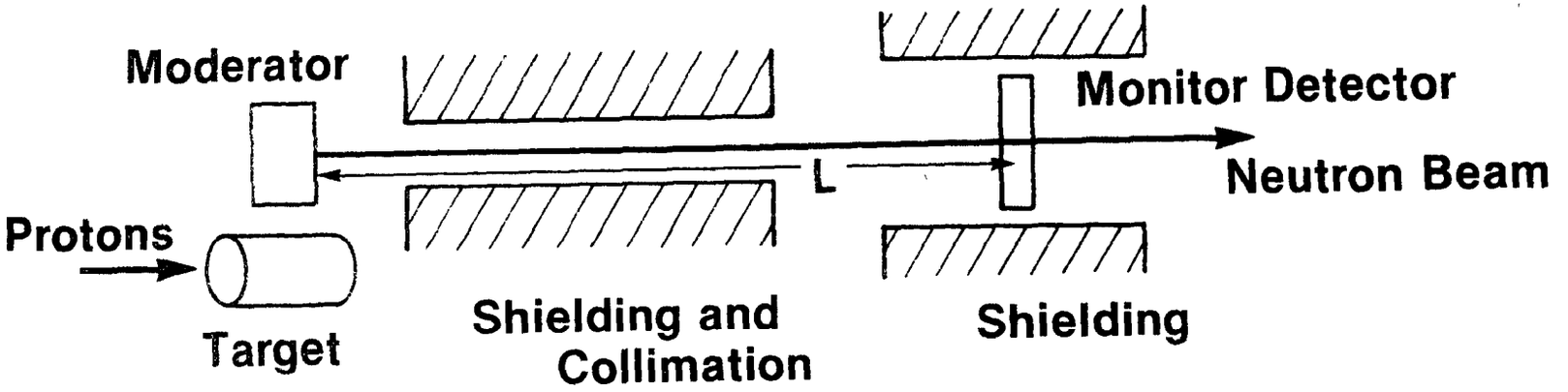

4. Schematic arrangement of the beam monitor detectors used in measuring the spectra.

$$C(t) = \int_0^\infty \eta(E')\Phi(E')\delta(t - L/v')dE' + B = A\eta(E)\Phi(E)(2E/t) + B \qquad (3)$$

where A is the area and $\eta(E)$ is the efficiency of the detector, and $\Phi(E)$ is the time-average flux per unit energy at the detector position. $v = L/t$ is the neutron speed and $E = \frac{1}{2}mv^2$ is the neutron energy corresponding to time t; the related wavelength is $\lambda = h/mv$. The time-average counting rate in a time-of-flight channel of width Δt centered at time t is $C(t)\Delta t$.

We represent $\Phi(E)$ by a Maxwellian function at longer wavelengths, joined smoothly to a 1/E "slowing-down" spectrum at shorter wavelengths,[3]

$$\Phi(E) = \Phi_{MB}(E) + \Phi_{SD}(E) \qquad (4)$$

where $\Phi_{MB}(E) = \Phi_{Th}(E/E_T^2)\exp(-E/E_T)$ (5)

represents the Maxwellian part of the spectrum. $E_T = k_B T_{eff}$ is the mean thermal energy, related to the effective temperature T_{eff}, which is usually somewhat greater than the physical temperature of the moderator medium. Φ_{Th} is the integrated Maxwellian flux,

$$\Phi_{Th} = \int_0^\infty \Phi_{MB}(E)dE, \qquad (6)$$

since $\int_0^\infty (E/E_T^2)\exp(-E/E_T)\, dE = 1$.

Polyethylene

The slowing-down part representing the room-temperature polyethylene spectrum is

$$\Phi_{SD}(E) = \Phi_{epi}(1/E)\Delta(E)(E/E_{ref})^{\alpha}. \qquad (7)$$

where the last factor represents the effect of leakage from the medium, and α is called the "leakage exponent". We take E_{ref} = 1000. meV for our purposes. The factor $\Delta(E)$ is the "joining function". Different authors have used several different forms; we used a generalized form of Westcott's[4] joining function,

$$\Delta(E) = [1 + (E_{co}/E)^s]^{-1} \qquad (8)$$

where the cutoff energy E_{co} is ordinarily about

$$E_{co} \simeq 5E_T, \tag{9}$$

and we designate the exponent s the "cutoff exponent". Westcott found the value s = 7 for the spectra he treated. Φ_{epi} is the epithermal neutron flux; assuming $\Phi_{Th}(E_{ref}) = 0.$ and $\Delta(E_{ref}) = 1.$,

$$\Phi_{epi} = [E\Phi(E)]\Big|_{Eref} \tag{10}$$

The detector efficiency was taken to be of the form

$$\eta(E) = K/\sqrt{E}, \tag{11}$$

where K is an unknown constant.

The parameter B represents the delayed neutron background, assumed constant over the time interval between pulses T = 1/f. If δ is the fraction of all neutrons which appear delayed then B represents the counting rate due to a steady source with a spectrum effectively identical to that characterizing the prompt pulse,

$$B = \delta/T \int_o^{Emax} \eta(E)\Phi(E)dE = \Phi_{epi}(\delta/T)F(\Phi_{Th}/\Phi_{epi}, E_T, s, E_{co}, \alpha, E_{max}), \tag{12}$$

so that

$$B/\Phi_{epi} = (\delta/T)F(\Phi_{Th}/\Phi_{epi},\ E_T\ s,\ E_{co},\ \alpha,\ E_{max}). \tag{13}$$

The ratio of the delayed neutron background to the epithermal flux is completely determined if the shape of the prompt spectrum is known, as in our empirical fitting function. We develop the required integral F in the Appendix.

It is interesting to note that, assuming no frame overlap C(t) = 0 for t > T, (the result is true without this assumption)

$$\int_o^T C(t)dt = \int_o^\infty A\eta(E)\Phi(E)dE + BT, \tag{14}$$

then

$$\int_o^T C(t)dt = BT\ \delta/(1 + \delta), \tag{15}$$

so that B is proportional to the integral of the counting rate over the entire frame

$$B = 1/T\ \delta/(1+\delta)\ \int_0^T C(t)dt. \tag{16}$$

Methane

The lower physical temperature of the solid methane moderator places the Maxwellian part of the spectrum roughly 20 times lower than that for the room-temperature polyethylene moderator. This exposes a slight "bump" in the slowing-down part of the spectrum which must be fitted in another way. In this case we described the slowing-down part by,

$$\Phi_{SD}(E) = \Phi_{epi}(1/E)\Delta_1(E)\Delta_2(E) \tag{17}$$

where $\Delta_1(E)$ is the same function used in the fitting of the polyethylene moderated neutron spectrum and $\Delta_2(E)$ is the "bump" function,

$$\Delta_2(E) = 1 + A\exp[-(E^p - E^p_B)^2/2\sigma^2] \tag{18}$$

where E_B is the bump energy, and σ represents the width of the bump. We found that the best fit was obtained with $p = -2/3$, which value we fixed during the least squares analysis. Both Westcott[4] and Mildner et al[5] have found it necessary to describe "bumps" in certain spectra.

Attenuation Corrections

We made no corrections for attenuation due to the presence of air and of aluminum windows between the source and the detector in the polyethylene spectrum. In the solid methane spectrum, we corrected the original data for the combined attenuation effects of the air and aluminum neutron cross sections. The neutron beam passed through 2.82m of air at atmospheric pressure and 0.5in. of aluminum in the solid methane measurement. To account for the attenuation due to this air, we used functions fitted to "Barn book" data for oxygen and nitrogen:

$$\sigma^{O_2}(E) = 3.77(1 + (15.5/E_{meV})^{1.762})^{0.222} \tag{19a}$$

$$\sigma^{N_2}(E) = 10.95(1 + (22.1/E_{meV})^{1.762})^{0.222} \tag{19b}$$

giving a total macroscopic cross section:

$$\Sigma_{total}(E) = 2N_A(0.78\sigma^N(E)+0.21\sigma^O(E))/V_m \quad (20)$$

where N_A is Avogadro's number and V_m is the STP molar volume.

We represented the aluminum cross section in terms of the sum of elastic (Bragg) scattering for ideal polycrystal, with inelastic scattering at large and small k[6], in the vein of the treatment by Marshall and Lovesey.[7] Attenuation corrections were made in the original data enabling us to fit the data as an unattenuated spectrum, rather than making corrections for the attenuation during each iteration of the fitting function. Channel widths Δt were always 20 μsec, while the time ranges fitted varied having minimum times between 500 μsec and 1500 μsec. We made no corrections for resolution, since these are insignificant in the present measurements.

Table 3 shows the parameters used to quantify the changes in the time-average moderator spectra.

Table 3

Parameters for least-squares fitting of moderator spectra

Parameter		Initial values	
		CH_2	CH_4
ratio of thermal to epithermal flux	Φ_{Th}/Φ_{epi}	2.5	3.5
thermal energy	E_T	40. meV	2.0 meV
epithermal flux	Φ_{epi}	first data point	
leakage exponent	α	0.01	----
cutoff energy	E_{co}	180. meV	10.0 meV
cutoff exponent	s	7.	6.15
background	B	1/2 last data point	
bump function coefficient	A	----	0.44

bump energy	E_B	----	305.0 meV
sigma	σ	----	0.018

The values of the parameters were calculated from the recorded number of counts (not normalized) taken on the SEPD and SAD at IPNS. We developed a FORTRAN code for this purpose, using the CERN library code MINSQ[8,9] to perform the (nonlinear) least squares fitting of the parameters. The function minimized was the sum of squares of the deviations of the fitting function from the data, normalized to the square of the estimated error in the data at each point. Thus the minimized function has the χ^2 distribution with known expected value at minimum; our fits typically provided a value of χ^2 only twice the expected value, which for our data represents approximately 2% rms error. The Table gives initial estimates provided to the minimization calculation, although the user of the code can change any of these estimates at execution time.

Figure 5 shows a representative plot of the fitted spectrum function. Such plots typically produced quite good fits (χ^2 on the order of 3000 for a data set of about 1500 points and with 7 fitting parameters in the case of polyethylene, and slightly better in the solid methane with 10 fitting parameters).

Results

Polyethylene

We tracked the behavior of these parameters over the lifetime of both moderators used in IPNS. The polyethylene moderator, next-to-last installed in IPNS, was in place from October, 1983 until January, 1985, during which the target received 8×10^{20} 450 MeV protons. We examined a total of ten data sets chosen to represent roughly logarithmically-spaced intervals spread over the lifetime of the moderator, using the cumulative proton number N_p as a measure of the age of the moderator.

Among all the parameters the thermal-to-epithermal flux ratio varies most significantly, as shown in Figure 6. The function

$$\phi_{Th}/\Phi_{epi} = A\exp(-BN_p) + C\exp(-DN_p), \qquad (21)$$

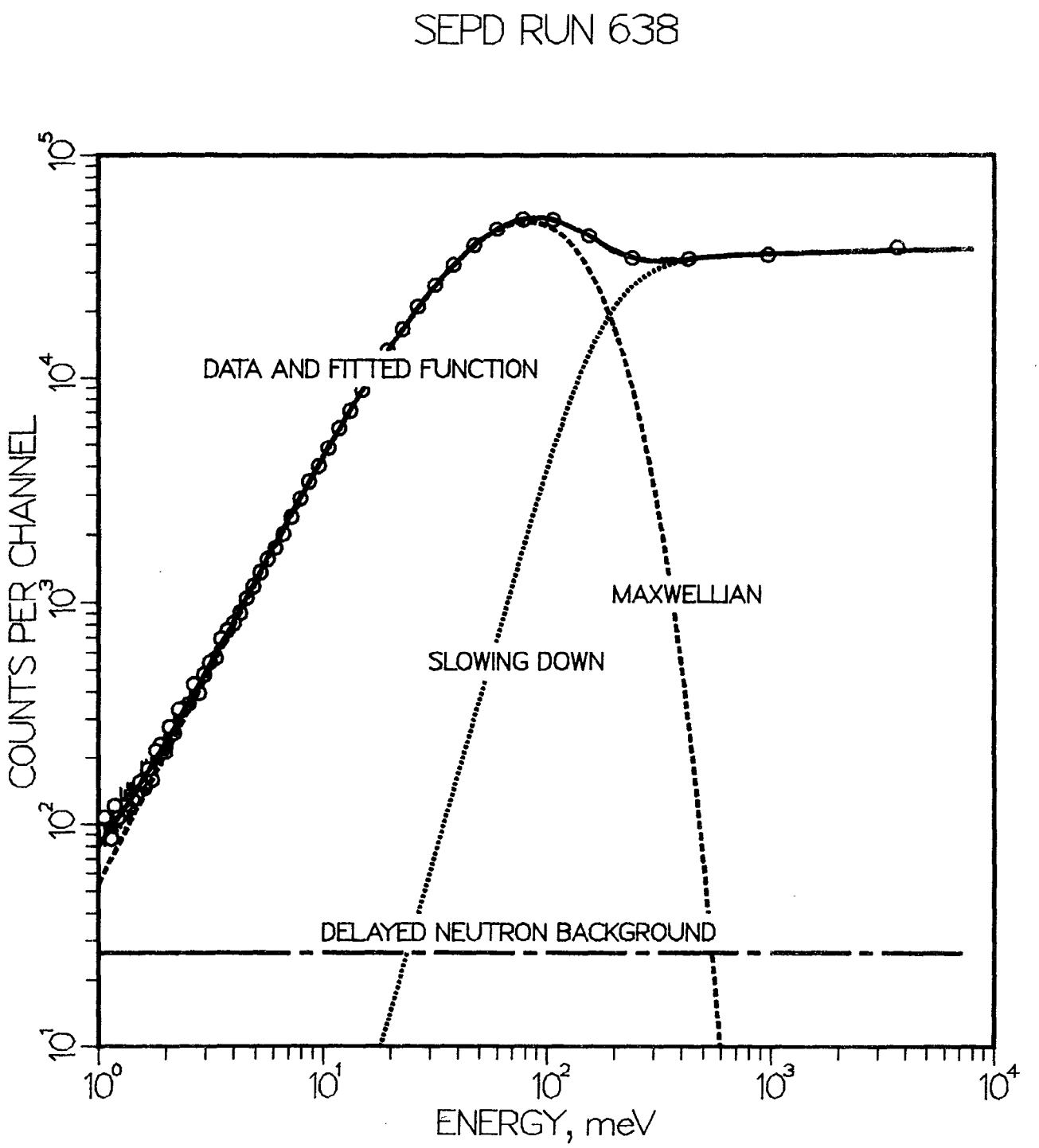

5. The counting rate distribution from the ambient temperature polyethylene moderator after 8.0 × 10^{20} 450 MeV proton irradiation of the IPNS target, as measured in a "1/v" detector. Circles represent every 25th data point. The various lines represent the Maxwellian and the slowing-down components and the time-independent delayed-neutron background.

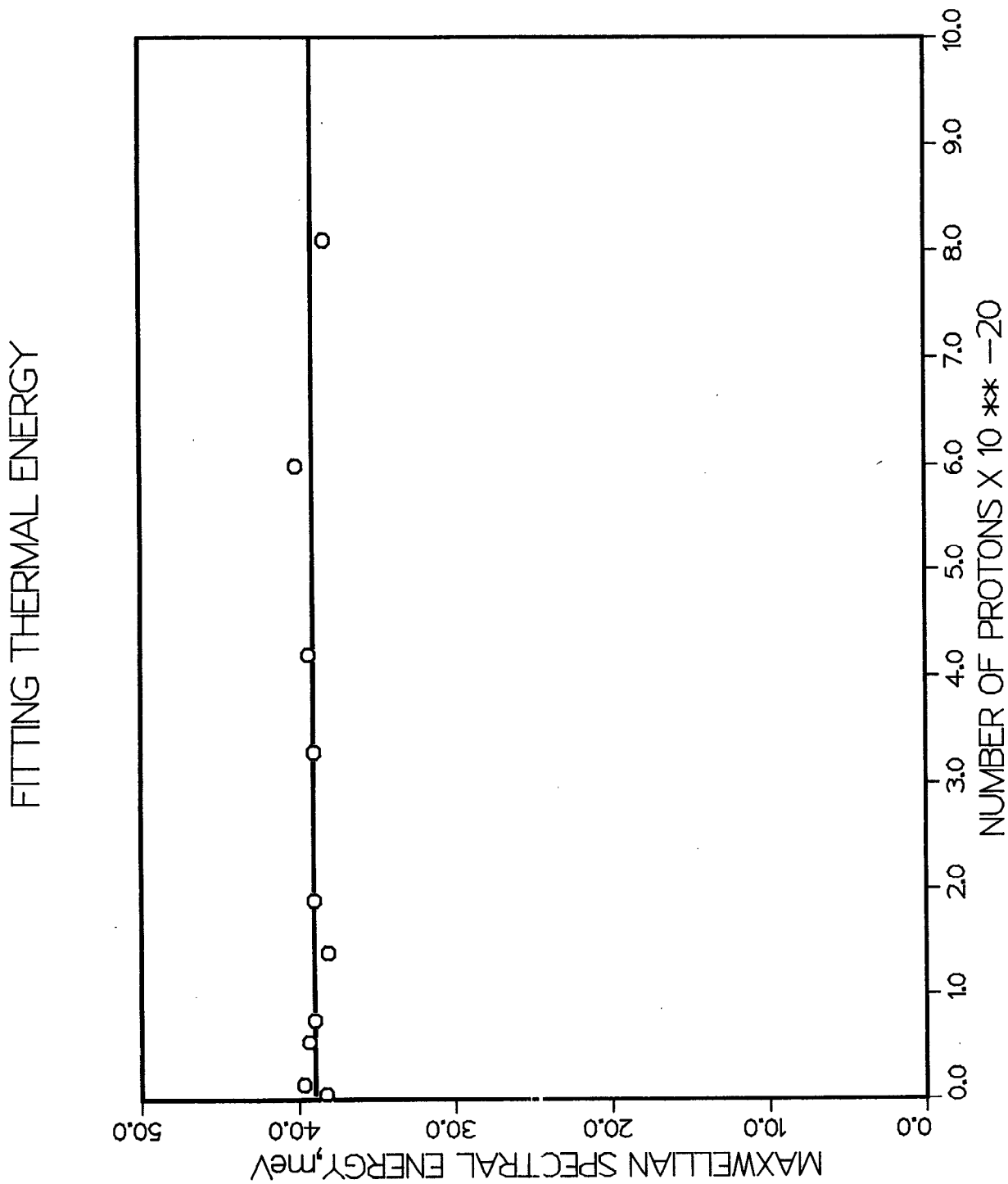

6. The thermal-to epithermal flux ratio ϕ_{Th}/Φ_{epi}, for polyethylene as a function of the number of protons on target.

shown as the solid line in Figure 6, fits the data reasonably well. Similarly, we have fitted the ratio of the epithermal flux to the proton current, Φ_{epi}/I_p to the function

$$\Phi_{epi}/I_p = A'\exp(-B'N_p) + C'\exp(-D'N_p). \quad (22)$$

Figure 7 shows the data and the fitted function. Table 4 summarizes the fitted parameters and estimated errors.

Table 4

Fitted Values of Parameters in ϕ_{Th}/Φ_{epi} and Φ_{epi}/I_p vs N_p

ϕ_{Th}/Φ_{epi}			Φ_{epi}/I_p		
A	0.740 ± 0.048	dimensionless	A′	0.584 ± 0.060	arbitrary units
B	$0.405 \pm 0.082 \times 10^{-20}$	protons^{-1}	B′	$0.356 \pm 0.083 \times 10^{-20}$	protons^{-1}
C	2.49 ± 0.078	dimensionless	C′	1.277 ± 0.042	arbitrary units
D	$0.0072 \pm 0.004 \times 10^{-20}$	protons^{-1}	D′	$0.0022 \pm 0.008 \times 10^{-20}$	protons^{-1}

We assert that D and D′ cannot be 0. in spite of their small values and low significance, since hydrogen still remains to be lost from the moderator (see Table 1.) The similarity of the coefficients B and B′, and D and D′ suggests that the same processes are responsible for the changes in both ϕ_{Th}/Φ_{epi} and Φ_{epi}/I_p. The physical significance of these functions is hidden behind the relationship of the ratios ϕ_{Th}/Φ_{epi} and Φ_{epi}/I_p to the material properties, and of the response of the material properties to irradiation.

The remaining five parameters changed only slightly over the lifetime of the polyethylene moderator; we fitted linear functions to their dependence on proton number:

$$E_T = 38.96(1. + 0.00024 \times 10^{-20} N_p) \quad (23)$$

$$E_{co} = 178.4(1. - 0.0072 \times 10^{-20} N_p) \quad (24)$$

$$s = 3.59(1. - 0.0295 \times 10^{-20} N_p) \quad (25)$$

$$\alpha = 4.5 \times 10^{-6}(1. - 0.049 \times 10^{-20} N_p) \quad (26)$$

The remarkable results are

7. The ratio of the epithermal neutron flux to the time-average proton beam current Φ_{epi}/I_p, for polyethylene as a function of the number of protons on target.

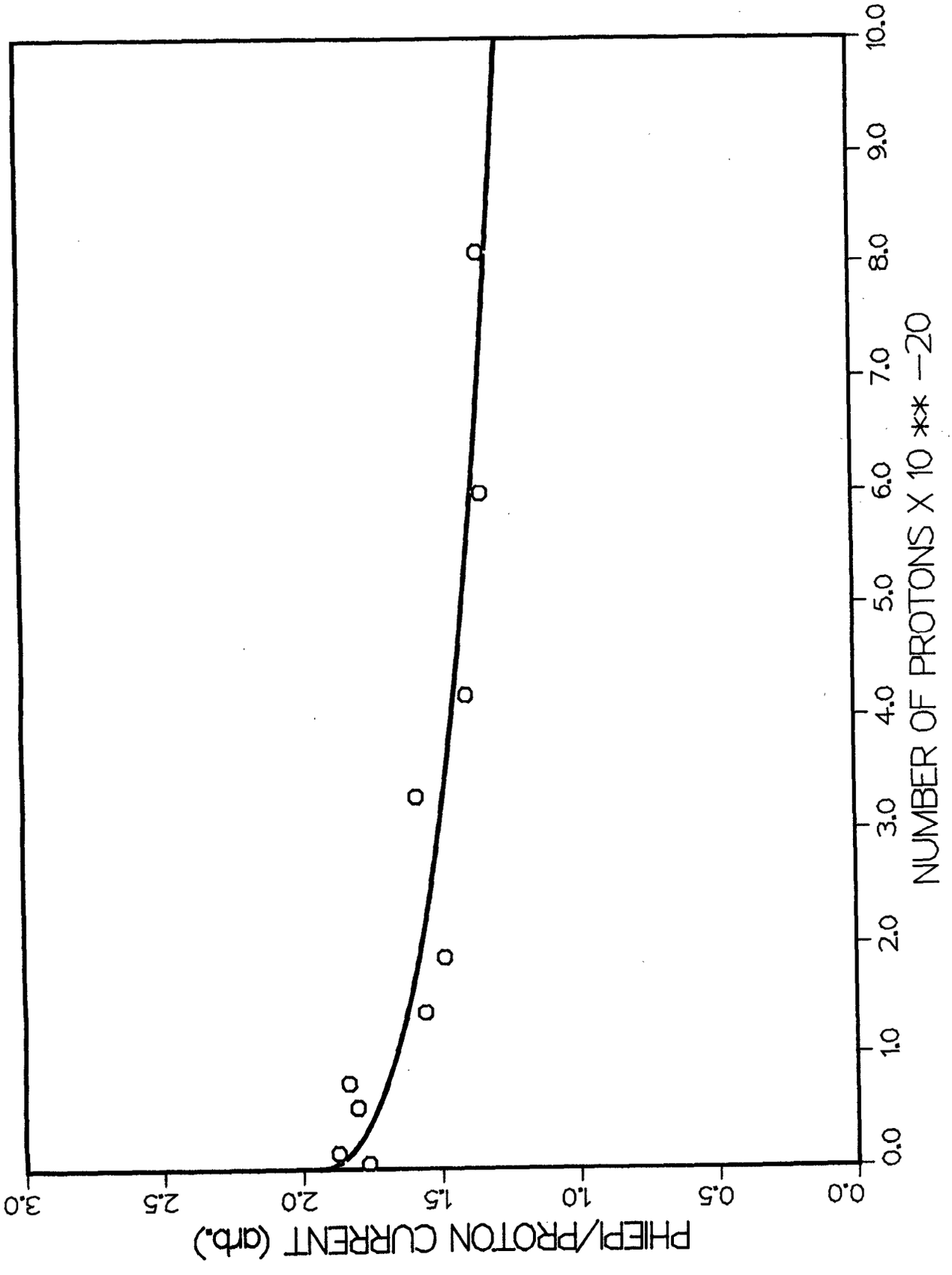

that the value of E_T varies so little, and that the leakage exponent is very small; presumably this is because the data do not extend to sufficiently high energy, so that the cutoff exponent takes up most of the non-1/E behavior.

Figure 8 shows the calculated ratio B/Φ_{epi} as a function of proton number, in which the best fit for the delayed neutron fraction is $\delta = .0024$, which is about 1/2 the value expected based on independent measurements. We attribute this error to the attenuation by materials in the beam path, which is not accounted for in the case of the polyethylene spectra, and to statistical imprecison in the fitted values of B.

Cold Solid Methane

We studied the performance of the solid methane moderator over a period of 21 days during which the target had received 1.23×10^{20} protons. During this period, we collected six spectra for study in order to relate the change in the fitting function parameters to the number of protons on target. Unlike those describing the polyethylene spectra, the parameters describing the solid methane spectra all displayed notable changes as the moderator aged. The ratio ϕ_{Th}/ϕ_{epi} changes significantly, as Figure 9 shows. The difference between the spectral temperture and the physical temperature shows a smooth, gradual increase with respect to the proton number as illustrated in Figure 10. We fitted the parameters of the fitting function either as a decaying exponential function or as a linear function of N_p, according to whether or not there seemed to be significant curvature in the relationship:

$$\Phi_{th}/\Phi_{epi} = 3.168(1 + 0.631 \exp(-5.596 \times 10^{-21} N_p) \quad (27)$$

$$\phi_{epi}/I_p = 9.295(1 + 0.0683 \exp(-1.037 \times 10^{-9} N_p)) \quad (28)$$

$$E_T - k_B T = 1.270(1 - 0.168 \exp(-2.067 \times 10^{-20} N_p)) \quad (29)$$

$$E_{co}/E_T = 4.699(1 - 2.351 \times 10^{-22} N_p) \quad (30)$$

$$s = 6.169(1 - 1.322 \times 10^{-21} N_p) \quad (31)$$

$$A = 0.542(1 - 0.188 \exp(-4.846 \times 10^{-20} N_p)) \quad (32)$$

$$E_B = 306.44(1 + 2.743 \times 10^{-21} N_p) \quad (33)$$

8. The ratio of the constant (delayed neutron) background to the epithermal neutron flux B/Φ_{epi}, for polyethylene as a function of the number of protons on target.

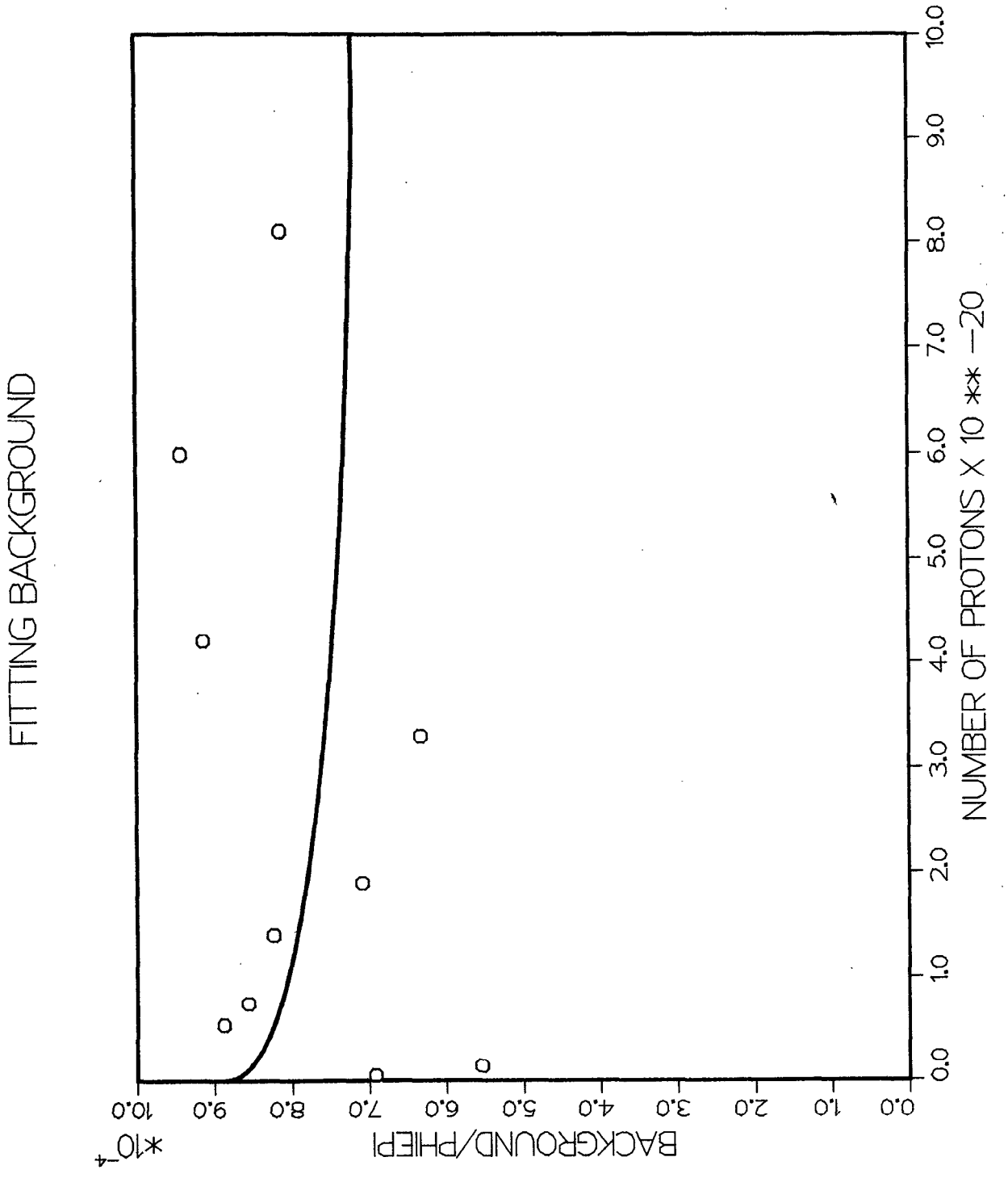

9. The thermal to epithermal flux ratio Φ_{th}/Φ_{epi}, for methane as a function of the number of protons on target.

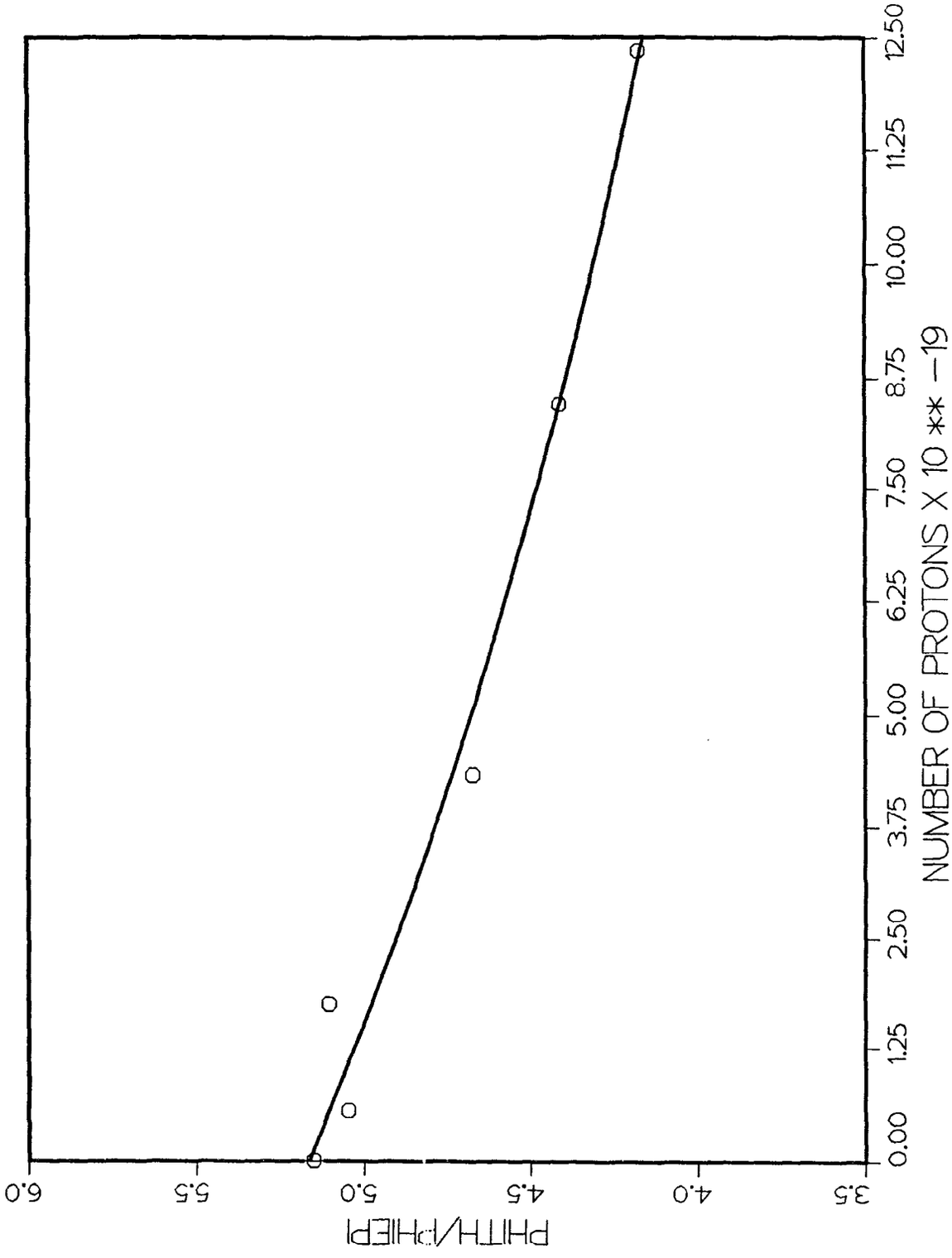

10. The difference between the spectral thermal energy and the physical thermal energy of the moderator $E_T - k_B T$, as a function of the number of protons on target.

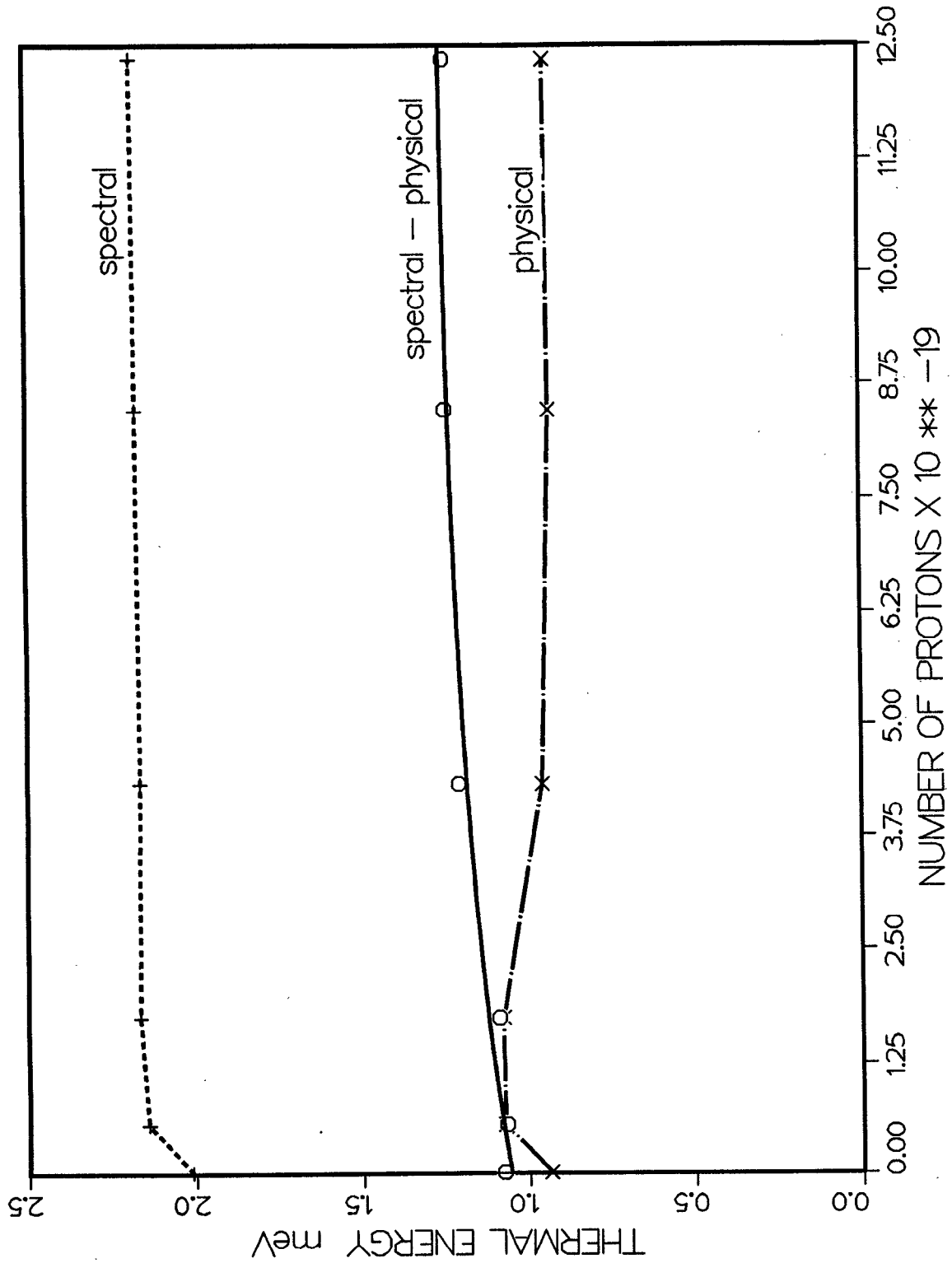

$$\sigma = 2.174(1 - .1805 \exp(-7.206 \times 10^{-21} N_p)) \quad (34)$$

That these changes in moderator performance have not been noted before may seem remarkable. However, IPNS is the first source having sufficient intensity to produce the large changes observed. The most-easily-determined parameter E_T happens to remain almost constant in both CH_2 and CH_4, so that only those instruments which record the spectrum well into the epithermal range and sense a change in the spectral shape could detect the change in the ratio Φ_{Th}/Φ_{epi}. Further, the deterioration seems to be about equally shared between the ratio Φ_{Th}/Φ_{epi} and the ratio Φ_{epi}/I_p (each 10-25 % for the range of doses we examined); the latter represents only a scale shift which can be overlooked in face of short term variations in accelerator current and changes in collimators and monitor detectors, and obscured by gradual improvement in accelerator current. Figures 11 and 12 show the fitted time-average spectra of the polyethylene and solid methane moderator at various stages of change due to irradiation. Although Φ_{epi}/I_p actually decreases with increasing N_p, the curves in Fig. 12 for larger N_p lie above those for smaller N_p due to variation of the shape and location of the bump.

Conclusions

We have quantified the radiation-induced changes in the time-average spectra from polyethylene and solid methane moderators irradiated in Argonne's Intense Pulsed Neutron Source, as a function of accumulated radiation dose. The polyethylene moderated spectra required a seven-parameter fit which describes the Maxwellian component and the slowing-down component of the intensity, and a constant delayed-neutron background. The fitting of the solid methane moderated spectra required a more involved function employing nine parameters. The functions fitted include a general form of Westcott's joining function and, in the case of the methane moderator, a function designed to fit the pronounced bump at roughly 200meV. These provide accurate representations of the spectra at all observed stages of irradiation. We have derived an expression for an integral of the fitted spectral function, which is useful to interpret the delayed-neutron background. The data reveal a significant decrease in the ratio of thermal to epithermal neutron fluxes during irradiation for both of the moderators. The mean thermal energy, and the cutoff energy and the cutoff exponent in the joining function vary only slightly as a function of accumulated dose. The leakage exponent describing the epithermal spectrum for polyethylene has very small values, presumably due to the fact that the data fitted did not extend to sufficiently high energies.

11. The ratio of the flux per unit lethargy to the instantaneous proton current, for the IPNS polyethylene moderator, as a function of neutron energy, at different stages of irradiation, N_p. The scale is arbitrary, but consistent for different values of N_p. From highest to lowest, the curves correspond to N_p = 0., 1., 4., 10., and 20. x 10^{20} protons on target.

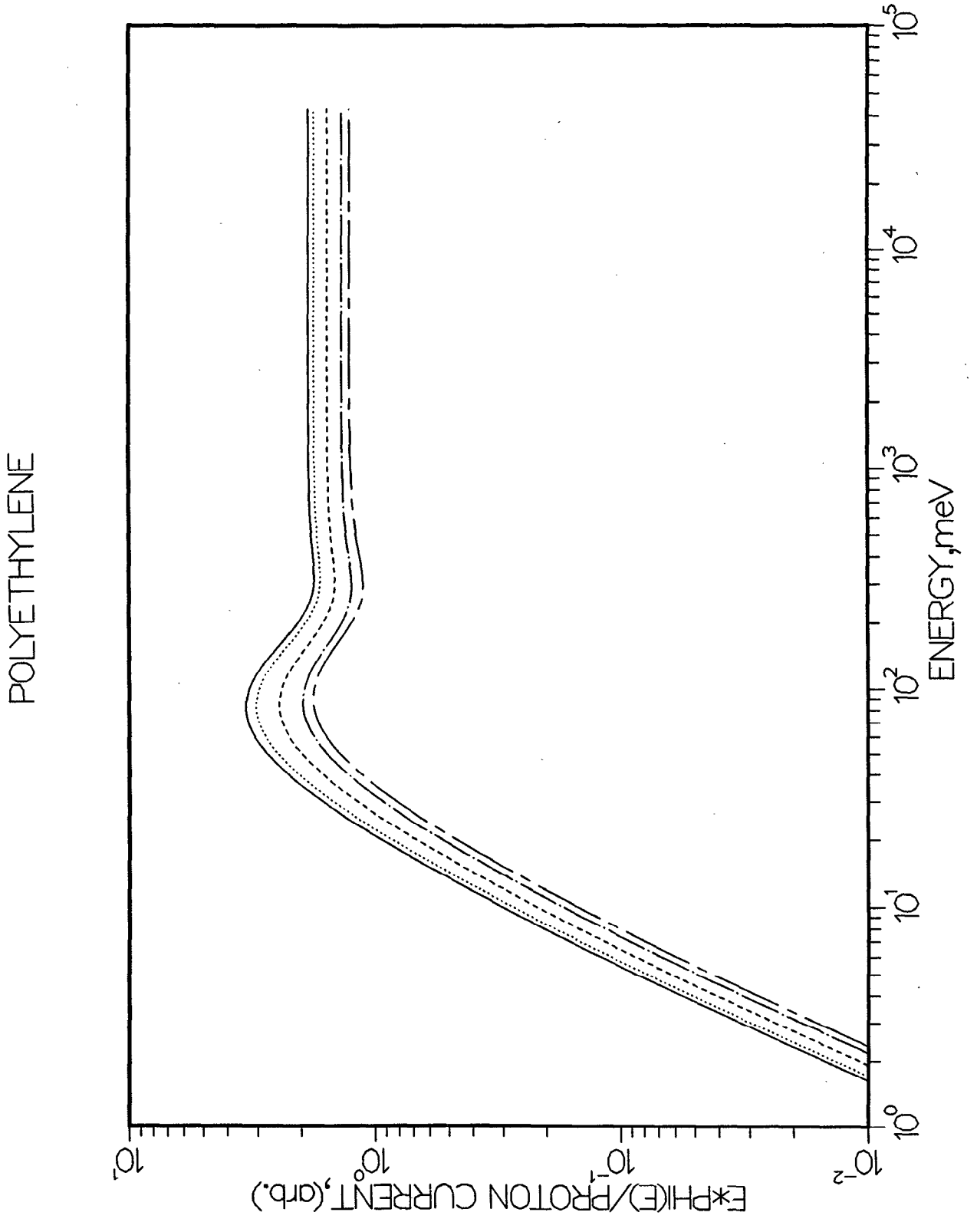

12. The ratio of the flux per unit lethargy to the instantaneous proton current, for the IPNS cold solid methane moderator, as a function of neutron energy, at different stages of irradiation, N_p. The physical temperature is assumed to be 12. K for these curves. The scale is arbitrary, but consistent for different values of N_p, and different from that of Fig. 11. From highest to lowest at low energies, the curves correspond to N_p = 0., 2., 6., 16., and 30. x 10^{19} protons on target.

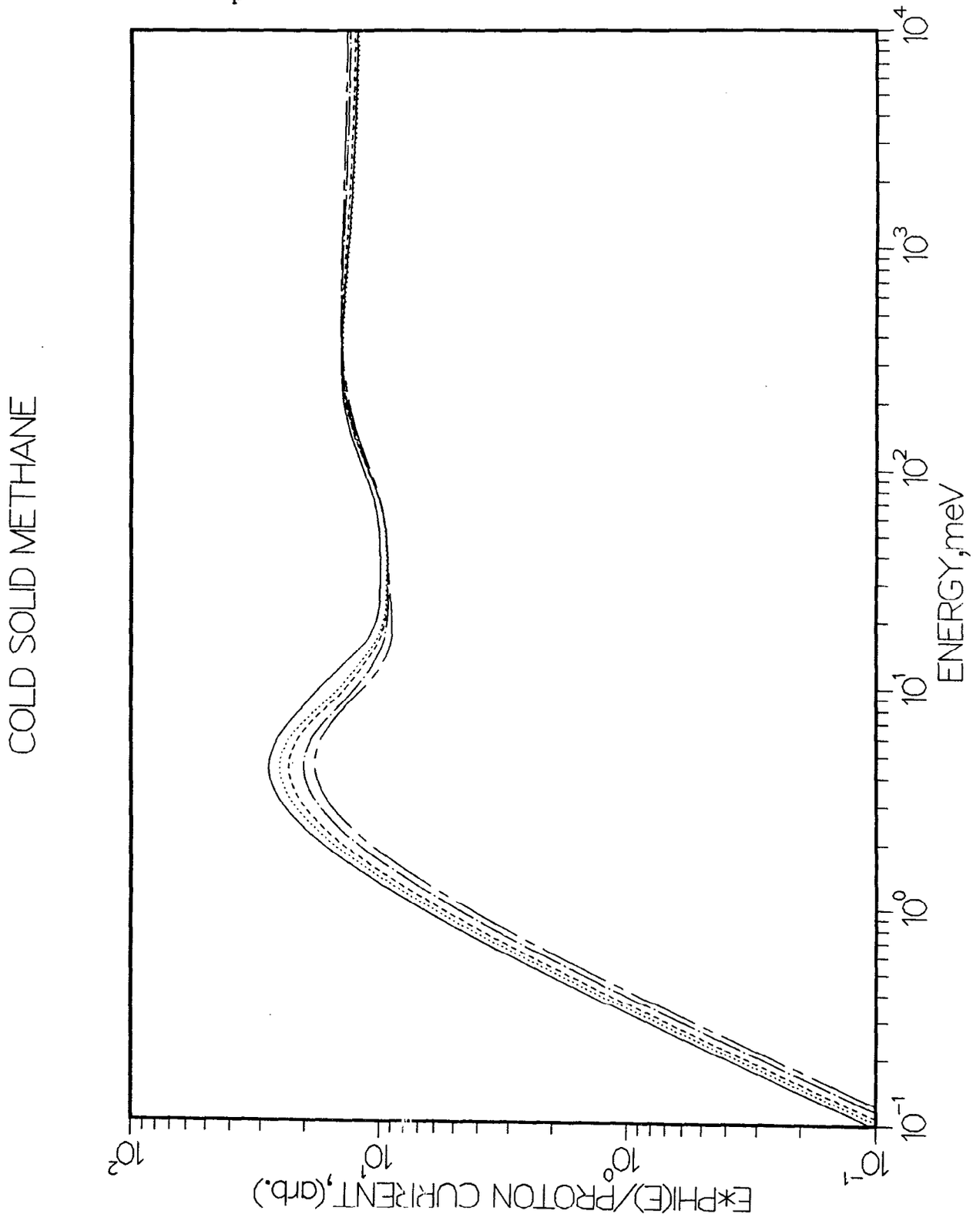

Acknowledgements

We thank F. J. Rotella and T. E. Klippert for their assistance in recovering archived data, and J. E. Epperson and D. L. Worcester for recording spectral data on the SAD. Two of us (SSC & CMD) express their gratitude to the Argonne Division of Educational Programs for support under the Student Research Participation Program.

REFERENCES

1. J. M. Carpenter, G. H. Lander and C. G. Windsor, "Instrumentation at Pulsed Neutron Sources", Rev. Sci. Instrum. 55 (7) 1984 1019.

2. J. M. Carpenter, A. W. Schulke, T. L. Scott, D. G. Wozniak, B. E. Benson and B. D. Leyda, "The IPNS Grooved, Solid Methane Moderator", Proceedings of the VIIIth Meeting of the International Collaboration on Advanced Neutron Sources (ICANS VIII), Oxford, U. K., 1985, to be published as a Rutherford-Appleton Laboratory report.

3. M. M. R. Williams, "The Slowing Down and Thermalization of Neutrons", North-Holland, 1967, p 89 ff. Also, K. H. Beckurts and K. Wirtz, "Neutron Physics", Springer, 1964, p 206.

4. C. H. Westcott, J. Nucl. Energy 2, (1955), 59; "Effective Cross Sections Values for Well-Moderated Thermal Reactor Spectra", Chalk River Report CRRP[A-960 (3^{d} Edition, Corrected), Nov., 1970.

5. D. F. R. Mildner, B. C. Boland, R. N. Sinclair, C. G. Windsor, L. J. Bunce and J. H. Clarke, Nucl. Instrum. Meth. 152 (1978) 437.

6. J. M. Carpenter, "A Simple Formula for the Total Cross Section of a Monatomic Polycrystal" IPNS Note 32, (Argonne internal report) 1986.

7. T. Pomentale, "Minimization of a Sum of Squares of Functions (MINSQ)", CERN Library subroutines.

8. M. J. D. Powell, "A Method for Minimizing a Sum of Squares of Non-Linear Functions Without Calculating Derivatives" Computer Journal 7, (1965), 303-307.

9. W. Marshall and S. W. Lovesey, "Theory of Thermal Neutron Scattering" Oxford, 1971.

Appendix

Calculation of the Delayed Neutron Background

We have fitted the function

$$\Phi(E) = \Phi_{MB}(E) + \Phi_{epi}(E)$$

to the time-average spectrum and wish the delayed neutron background

$$B = \delta/T \int_o^\infty A\eta(E)\Phi(E)dE = \Phi_{epi}\ \delta/T\ F.$$

The purpose of this Appendix is to compute the integral F in the above expression,

$$F = \Phi_{Th}/\Phi_{epi} \int_o^\infty (E^{1/2}/E_T 2)\exp(-E/E_T)dE + \int_o^{Emax} 1/(1 + (E_{co}/E)^S)E^{-3/2}(E/E_{ref})^\alpha dE,$$

where E_{max} is the energy ($\simeq$ 1 MeV) at which we assume the epithermal spectrum to go abruptly to zero, approximately representing the upper limit of the primary source spectrum. The first integral is easily recognized as a gamma function

$$\int_o^\infty (E^{1/2}/E_T 2)\exp(-E/E_T)dE = E_T^{-1/2}\Gamma(3/2) = \sqrt{\pi}/(2\sqrt{E_t}).$$

The second integral can be written

$$\int_o^{Emax} 1/(1 + (E_{co}/E)^S)E^{-3/2}(E/E_{ref})^\alpha dE = \sqrt{E_{co}}(E_{co}/E_{ref})^\alpha\ f,$$

where f is identifiable as an incomplete Beta function. We need not appeal to this relationship, except to note that the integral converges for $\alpha < 1/2$ when E_{max} is finite. It is convenient to express

$$f = \int_o^\infty x^{-1/2-\alpha}/(1 + x^S)dx - \int_o^{xmin} x^{-1/2-\alpha}/(1 + x^S)dx,$$

with $x = E_{co}/E$ and $x_{min} = E_{co}/E_{max}$. This form requires the additional condition $s - \alpha > 1/2$. With the substitution

$$y = x^S$$

the first term is recognizable as a standard integral,

$$1/s\int_o^\infty y^{(1/2-\alpha)/s-1}/(1 + y)dy = (\pi/s)/\sin[\pi(1/2 - \alpha)/s].$$

Since x_{min} in the second term is very small, we approximate the integral to lowest order in x_{min},

$$\int_o^{xmin} x^{-1/2-\alpha}/(1 + x^S)dx \simeq 2x_{min}^{(1/2-\alpha)}/(1 - 2\alpha),$$

so that

$$f \simeq (\pi/s)/\sin[\pi(1/2 - \alpha)/s] - 2x_{min}^{(1/2-\alpha)}/(1 - 2\alpha).$$

It is instructive to note that for small values of $\pi(1/2 - \alpha)/s$,

$$(\pi/s)/\sin[\pi(1/2 - \alpha)/s] \simeq 2/(1 - 2\alpha),$$

which is the result for an abrupt ($s \to \infty$) cutoff at $E = E_{co}$.

Thus finally,

$$F = \Phi_{Th}/\Phi_{epi}\sqrt{\pi}/(2\sqrt{E_T}) + 2/\sqrt{E_{co}}(E_{co}/E_{ref})^{\alpha}f,$$

and

$$B/\Phi_{epi} = (\delta/T)F.$$

These results for $\alpha \neq 0$ seem not to have been worked out before, although the present result is similar in content to Westcott's (g+rs) for a "1/v" absorber.